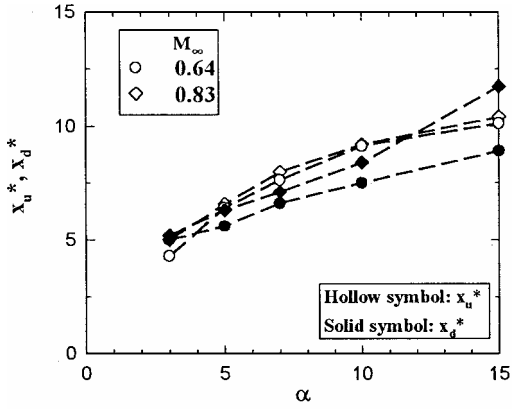

a)

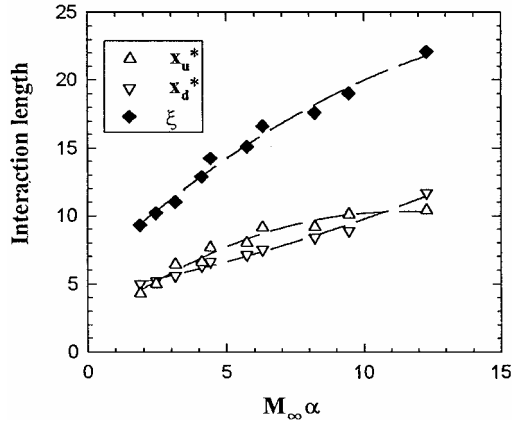

b)

Fig. 2 Interaction region.

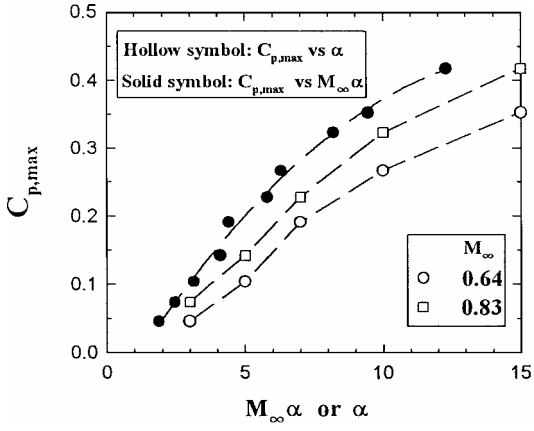

Fig. 3 Peak pressure.

other hand, the scaling parameter $M_\infty\alpha$ is more suitable (Fig. 2b). The upstream influence appears to be a quadratic function of $M_\infty\alpha$, and the correlation of the downstream influence and $M_\infty\alpha$ is also reasonably good. The extent of the interaction region shows a similar trend as the upstream and downstream influences. A good collapse of the data with $M_\infty\alpha$ can be seen.

The peak pressure downstream of the corner can be used to characterize the strength of the upstream compression processes. In Fig. 3 it can be seen that the peak pressure downstream of the concave corner can also be scaled with $M_\infty\alpha$. Stronger compression is associated with increasing freestream Mach number and concave-corner angle. Note that the peak pressure at $M_\infty\alpha = 12.30$ increases up to 42% of dynamic pressure.

Conclusions

Experiments were carried out to study the characteristics of compressible concave-corner flows. The surface-pressure distributions show similar characteristics for all of the test cases. The flows decelerate upstream of the corner and accelerate downstream of the corner. Stronger upstream compression and downstream expansion are observed with increasing Mach number and concave-corner angle, which induce a larger interaction region. The similarity parameter $M_\infty\alpha$ appears to be a suitable scaling parameter to characterize the compressible concave-corner flows, which include the interaction region (upstream and downstream influences) and the upstream compression (peak pressure).

Acknowledgments

The research was support by National Science Council (NSC 90-2212-E-006-132). The support is gratefully acknowledged. The author also thanks the technical support of the Aerospace Science and Technology Research Center/National Cheng-Kung University technical staffs with the experiments.

References

[1]Rajeswari, B., and Prabhu, K. R., "Optimum Flap Schedules and Minimum Drag Envelopes for Combat Aircraft," *Journal of Aircraft*, Vol. 24, No. 4, 1987, pp. 412–414.

[2]Bolonki, A., and Gilyard, G. B., "Estimated Benefits of Variable-Geometry Wing Camber Control for Transport Aircraft," NASA TM-1999-206586, Oct. 1999.

[3]Szodruch, J., and Hilbig, R., "Variable Wing Camber for Transport Aircraft," *Progress in Aerospace Science*, Vol. 25, No. 3, 1988, pp. 297–328.

[4]Chung, K., "Transition of Subsonic and Transonic Expansion Flows," *Journal of Aircraft*, Vol. 37, No. 6, 2000, pp. 1079–1082.

[5]Lu, F. K., "Fin Generated Shock-Wave Boundary Layer Interactions," Ph.D. Dissertation, Mechanical Engineering, Penn State Univ., PA, May 1988.

Optimum Downwash Behind Wings in Formation Flight

James W. Frazier* and Ashok Gopalarathnam†
North Carolina State University, Raleigh, North Carolina 27695

Nomenclature

b	=	aircraft wing span
C_{Di}	=	aircraft-induced drag coefficient
C_L	=	aircraft lift coefficient
C_l	=	local section lift coefficient
c	=	local chord
D	=	aircraft induced drag
$\boldsymbol{I}$	=	influence coefficient matrix of size $n \times n$
L	=	aircraft lift
n	=	number of horseshoe vortices on all of the aircraft
P, Q	=	constants used in defining downwash distribution
R	=	aircraft rolling moment
V_∞	=	freestream velocity
w	=	Trefftz-plane downwash

Received 3 October 2002; revision received 8 February 2003; accepted for publication 9 February 2003.

*Graduate Research Assistant, Department of Mechanical and Aerospace Engineering, Box 7910; currently Student Test Pilot Officer, U.S. Naval Test Pilot School, Patuxent River, MD 20670.

†Assistant Professor, Department of Mechanical and Aerospace Engineering, Box 7910; ashok_g@ncsu.edu. Member AIAA.

$\boldsymbol{w}$ = vector containing the n Trefftz-plane downwash values
w = downwash at quarter-chord
X = streamwise separation between adjacent aircraft
Y = centerline-to-centerline lateral separation between adjacent aircraft
y = spanwise coordinate
Γ = bound vorticity strength
$\boldsymbol{\Gamma}$ = vector of the n bound vortex strengths
γ = perturbation to bound vorticity
Λ = quarter-chord sweep
ρ = density of air

Subscripts

A = aircraft A
av = average
B = aircraft B

Superscripts

l = left wing tip
m = centerline of aircraft
r = right wing tip

Introduction

IT is well known that formation flight has the potential to offer significant induced drag reductions. The analytical work of Lissaman and Shollenberger,[1] as well as the recent experimental measurements on birds in flight,[2] both show that birds achieve significant energy savings in formation flight when compared to solo flight. With advances in precision measurement and control of relative position, formation flight is receiving increased interest for aircraft drag reduction, for example, Ref. 3.

Birds are able to take advantage of their variable-geometry wings to achieve near-optimum spanwise lift distributions. In contrast, aircraft with rigid wings have less flexibility in adapting the wing geometry for maximizing the formation flight benefits. Use of adaptive lifting surfaces may enable future aircraft to take full advantage of formation flying benefits. It is, therefore, worthwhile to explore approaches that can determine the optimum lift distributions on wings in formation flight. These approaches also provide the lower limit in induced drag attainable for any given formation geometry. In a recent work, Iglesias and Mason[4] have presented a constrained-minimization approach using Lagrange multipliers for determining the optimum lift distribution on aircraft flying in formation. This optimum lift distribution results in minimum induced drag for the entire formation while satisfying the constraints that the lift on each aircraft equals the weight and the individual rolling moments are all zero. This optimum lift distribution and the formation induced drag are independent of the streamwise spacing of the aircraft.

In the current work, which was inspired by Ref. 4, an alternate approach is presented for determining the optimum lift distribution, that is, by first determining the optimum downwash distribution in the Trefftz plane (the plane normal to V_∞ and located at downstream infinity). Such approaches have been used earlier for single wings flying in isolation.[5–7] The advantage of such an approach is that it often results in a simple and elegant analytical result for the shape of the Trefftz-plane downwash distribution. For example, Munk's classic work[5] showed that a nonplanar wing having minimum induced drag must have a lift distribution such that the downwash along the wake trace in the Trefftz plane is proportional to the cosine of the local wing dihedral angle. For a planar wing, this result turns out to be constant spanwise downwash, and the associated lift distribution is the well-known elliptic distribution.

The current work uses the calculus-of-variation approach of Jones[6] to determine the optimum downwash behind wings in formation flight. As with the work of Ref. 4, the wake is assumed to be rigid and invariant with the streamwise direction, and it is assumed to trail behind the wings in the direction of the freestream. The aim is to find the downwash distribution behind the wings such that the total induced drag of the entire system of wings is a minimum while satisfying the constraints on the desired lift and desired zero rolling moment on each wing. A vortex lattice formulation is then used to determine the optimum lift distributions from the optimum downwash using a numerical approach similar to that described by Blackwell.[8] The drag of the individual aircraft is obtained from a near-field analysis as described by Iglesias and Mason.[4] In the following section, first the theory is described. Results are then presented for lift and downwash distributions for wings in formation flight.

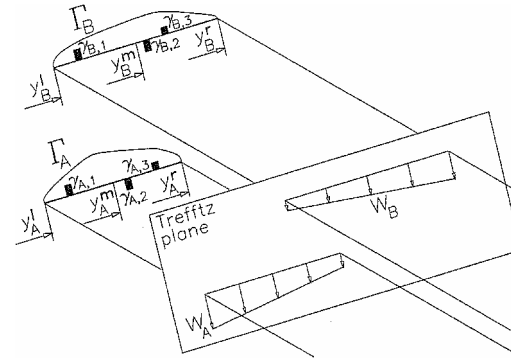

Fig. 1 Loading and Trefftz-plane downwash for the two-aircraft example.

Approach

Optimum Downwash

To illustrate the approach, two aircraft flying in close formation are considered. The aircraft need not be identical. It is assumed that the two aircraft, A and B, are optimally loaded, that is, the lift distributions on the two aircraft are such that the total induced drag of the formation is a minimum, the total lift on each aircraft equals the corresponding weight, and the rolling moment about the center of gravity for each aircraft is zero. This lift distribution, referred to as the original lift distribution, is shown schematically in Fig. 1.

If $\Gamma_A(y)$ and $\Gamma_B(y)$ are the bound vortex distributions associated with the original lift distributions on the two aircraft A and B, then the lift L_A and L_B on each aircraft can be can be computed by spanwise integration, as shown in Eq. (1) using aircraft A as example. The aircraft rolling moment R due to the lift distribution can also be computed from the Γ distribution and is shown in Eq. (2) for aircraft A. Furthermore, when the Trefftz-plane downwash distributions $w_A(y)$ and $w_B(y)$ are used, the total induced drag of the entire formation with this lift distribution can be readily computed, as shown in Eq. (3). Note that the induced drag for each of the individual aircraft cannot be determined from the Trefftz-plane downwash and has to be computed from a near-field method, as pointed out in Ref. 4. With aircraft A used as an example, if the lift distribution on the wing is modeled using a bound vortex of varying strength $\Gamma_A(y)$ along the quarter-chord line with local sweep angle $\Lambda(y)$ and $w_A(y)$ is the downwash distribution along this line, then the induced drag of aircraft A is given by Eq. (4). The effect of sweep is automatically taken into account in Eq. 4 because the integration is performed along the spanwise coordinate y and not along the quarter-chord line. Thus,

$$L_A = \rho V_\infty \int_{y_A^l}^{y_A^r} \Gamma_A(y)\,\mathrm{d}y \tag{1}$$

$$R_A = -\rho V_\infty \int_{y_A^l}^{y_A^r} \Gamma_A(y)\left(y - y_A^m\right)\mathrm{d}y \tag{2}$$

$$D = \frac{\rho}{2}\left[\int_{y_A^l}^{y_A^r} w_A(y)\Gamma_A(y)\,\mathrm{d}y + \int_{y_B^l}^{y_B^r} w_B(y)\Gamma_B(y)\,\mathrm{d}y\right] \tag{3}$$

$$D_A = \rho \int_{y_A^l}^{y_A^r} w_A(y)\Gamma_A(y)\,\mathrm{d}y \tag{4}$$

As noted by Jones,[6] if the induced drag is to be a minimum, then a small variation in the shape of the lift distribution will produce no first-order change in the formation induced drag. Additionally, if the constraints on the individual lift and rolling moment are to be satisfied, then the small variation in the lift distribution should produce no change in the individual aircraft lift and rolling moment. The change in the formation induced drag due to a small variation in the Γ distribution (referred to as additional distribution) is composed of three parts[6]: 1) the drag arising from the additional Γ distribution acting on the additional Trefftz-plane downwash distribution, 2) the drag arising from the original Γ distribution acting on the additional Trefftz-plane downwash distribution, and 3) the drag arising from the additional Γ distribution acting on the original Trefftz-plane downwash distribution. The first part is a second-order term and can be neglected when compared to the other two parts. From Munk's mutual drag theorem,[5] the second and third parts of the additional induced drag are equal. Therefore, if the first-order change in formation induced drag is to be zero, then it is sufficient to set the drag arising from the additional Γ distribution acting on the original Trefftz-plane downwash distribution (third part) to zero.

To satisfy the constraints on the specified lift and zero rolling moment for each aircraft, the additional Γ distribution should be selected such that it generates no additional lift or rolling moment for each of the aircraft. It can be seen that such an additional Γ distribution for each aircraft must have at least three elements to satisfy these two constraints. Furthermore, using the arguments of Jones,[6] any additional distribution meeting these requirements can be subdivided into groups of three elements, so that each individual group independently satisfies the constraints. Therefore, as representative of perturbation curves that satisfy the constraints, the additional Γ distribution can be represented using three small elements on each wing. This additional Γ distribution is shown in Fig. 1 along with the original Γ distribution for the two aircraft. For instance, aircraft A has an additional distribution composed of three elements with areas $\gamma_{A,1}$, $\gamma_{A,2}$, and $\gamma_{A,3}$ in Fig. 1 and have been arbitrarily located at $y_{A,1}$, $y_{A,2}$, and $y_{A,3}$.

If the original Γ distribution represents the optimum loading, then the additional Γ distribution must satisfy the following three conditions: 1) There should be no change in the lift on aircraft A and B [Eqs. (5) and (6)]. 2) There should be no change in the rolling moments [Eqs. (7) and (8)]. 3) There should be no change in the total induced drag [Eq. (9)]. In Eq. (9), $w_{A,1}$, $w_{A,2}$, and similar terms are the Trefftz-plane downwash values associated with the original Γ distribution at the corresponding locations $y_{A,1}$, $y_{A,2}$, and so on. Therefore,

$$\gamma_{A,1} + \gamma_{A,2} + \gamma_{A,3} = 0 \tag{5}$$

$$\gamma_{B,1} + \gamma_{B,2} + \gamma_{B,3} = 0 \tag{6}$$

$$\gamma_{A,1}\left(y_{A,1} - y_A^m\right) + \gamma_{A,2}\left(y_{A,2} - y_A^m\right) + \gamma_{A,3}\left(y_{A,3} - y_A^m\right) = 0 \tag{7}$$

$$\gamma_{B,1}\left(y_{B,1} - y_B^m\right) + \gamma_{B,2}\left(y_{B,2} - y_B^m\right) + \gamma_{B,3}\left(y_{B,3} - y_B^m\right) = 0 \tag{8}$$

$$\gamma_{A,1}w_{A,1} + \gamma_{A,2}w_{A,2} + \gamma_{A,3}w_{A,3} + \gamma_{B,1}w_{B,1} + \gamma_{B,2}w_{B,2} + \gamma_{B,3}w_{B,3} = 0 \tag{9}$$

Note that to satisfy Eqs. (5–9), the original Trefftz-plane downwash along the wake trace of each wing must be of the form $w_A(y) = P_A + Q_A(y - y_A^m)$ and $w_B(y) = P_B + Q_B(y - y_B^m)$, where P_A, Q_A, P_B, and Q_B are constants that are determined using the values of the specified lift L_A and L_B and the rolling moments R_A and R_B for the two aircraft. In the current problem, R_A and R_B are both zero.

Although the method has been illustrated using two aircraft, the result can be generalized for any arbitrary number of wings in formation flight and can be stated as follows: The lift distributions for wings in formation flight with constraints on the lift and rolling moment on each wing must result in a linear variation in the Trefftz-plane downwash for the total induced drag of the formation to be a minimum. That the condition for minimum induced drag can be summarized in such a simple statement even for a complex configuration of multiple wings points to the elegance of the optimum-downwash approach pioneered by Munk[5] and Jones.[6]

The current formulation is valid only for formation geometries in which the wake traces of the wings in the Trefftz plane do not intersect or overlap with each other. If the wake traces of two wings have intersecting or overlapping wake traces, then they share the same Trefftz-plane downwash value at each of the common points of overlap. Because the current formulation does not account for such a constraint in the downwash, the method is restricted to wings that do not intersect or overlap in the front view. In any case, with wings having overlapping trailing-vortex wakes, the effects of viscosity and rollup of the wake[9] become important and need to be considered, although it may prove to be challenging to incorporate these considerations in the determination of optimum spanloads. These effects are not included in the current inviscid, rigid-wake formulation. These limitations are also applicable to the constrained-minimization approach of Ref. 4.

Optimum Lift Distribution

The Γ distributions on the wings and the associated Trefftz-plane downwash w distributions behind them are closely related and can be determined using a discrete vortex method similar to that described by Blackwell.[8] Briefly, the bound vorticity distribution on all of the wings and the trailing vorticity shed behind them are approximated using n horseshoe vortices, each having a constant value for the bound vortex strength Γ. With such a formulation, the n-dimensional $\boldsymbol{\Gamma}$ vector and the n-dimensional $\boldsymbol{w}$ vector can be related using an $n \times n$ influence coefficient matrix $\boldsymbol{I}$ as shown in Eq. (10). For a known $\boldsymbol{w}$, the $\boldsymbol{\Gamma}$ distribution can be computed by solving Eq. (10) and the lift, rolling moment, and drag can then be determined using Eqs. (1–4).

$$\boldsymbol{I} \cdot \boldsymbol{\Gamma} = \boldsymbol{w} \tag{10}$$

For the current problem, $w(y)$ for each aircraft is known in terms of the two unknown constants P and Q. These unknowns are computed using a single step of Newton's method as shown in Eq. (11) for the two-aircraft example used earlier in this section. The solution is made simple because zero values for the P and Q correspond to zero values for L and R. The Jacobian of the partial derivatives is computed using finite differencing. For example, $\partial L_A/\partial P_A$ is computed by making a small change to P_A and computing the change to L_A. The right-hand side is a vector of the desired values of lift L_A and L_B and rolling moments R_A and R_B. In the current problem, the rolling moments are set to zero. Thus, the P and Q can be determined using

$$\begin{pmatrix} \frac{\partial L_A}{\partial P_A} & \frac{\partial L_A}{\partial Q_A} & \frac{\partial L_A}{\partial P_B} & \frac{\partial L_A}{\partial Q_B} \\ \frac{\partial R_A}{\partial P_A} & \frac{\partial R_A}{\partial Q_A} & \frac{\partial R_A}{\partial P_B} & \frac{\partial R_A}{\partial Q_B} \\ \frac{\partial L_B}{\partial P_A} & \frac{\partial L_B}{\partial Q_A} & \frac{\partial L_B}{\partial P_B} & \frac{\partial L_B}{\partial Q_B} \\ \frac{\partial R_B}{\partial P_A} & \frac{\partial R_B}{\partial Q_A} & \frac{\partial R_B}{\partial P_B} & \frac{\partial R_B}{\partial Q_B} \end{pmatrix} \begin{pmatrix} P_A \\ Q_A \\ P_B \\ Q_B \end{pmatrix} = \begin{pmatrix} L_A \\ R_A \\ L_B \\ R_B \end{pmatrix} \tag{11}$$

This approach can be readily extended to a formation of more than two aircraft.

For a given formation of several wings with the geometry specified in the front view, known values for the specified lift, and zero rolling moments, the approach, thus, allows computation of the P and Q that in turn determine the Trefftz-plane downwash. The Γ distributions are then computed, from which other quantities can be determined. If in addition, the planform geometry of the entire formation is known, the induced drag for each individual aircraft can also be computed using the near-field approach[4] shown in Eq. (4) for aircraft A.

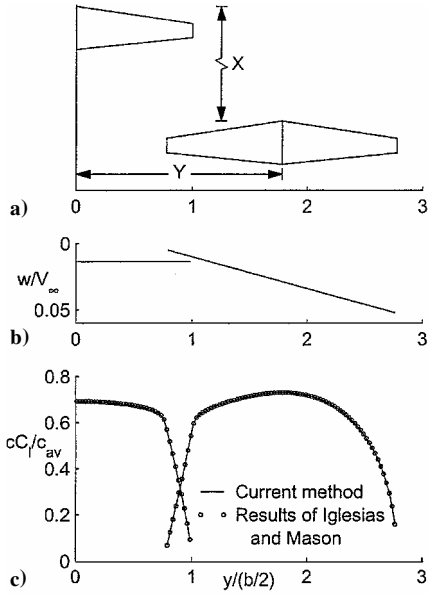

Fig. 2 Comparison of the optimum lift distribution with the results of Ref. 4: a) right-side plan view of the formation geometry, b) Trefftz-plane downwash distribution, and c) spanload distribution from the two methods.

Results

The current approach was used to determine the optimum downwash and lift distribution for three identical wings, each having an aspect ratio of 8, in symmetric formation flight. The geometry for this example is identical to one of the configurations used in Ref. 4 and has been used for validation of the current method. Figure 2a shows the right side of the plan view of the formation. There is a small vertical separation (1% span) between the middle lead aircraft and each of the corner wings and $Y = 0.89b$. Each aircraft is required to operate at C_L of 0.6 and to have zero rolling moment. Figure 2b shows the nondimensional Trefftz-plane downwash distribution w/V_∞ from the current method. It is seen that the middle aircraft has constant downwash because of the symmetry of the configuration. Figure 2c shows the excellent comparison between the resulting spanwise nondimensional lift distribution from the current method and that obtained by Iglesias and Mason.[4] The formation C_{Di}, defined as the total formation induced drag referenced to the total planform area of all of the wings, was determined to be 0.00707. If the three aircraft had been flying in isolation, their average C_{Di} would have been 0.01415, as predicted by the current vortex lattice method. This prediction for the solo flight C_{Di} is close to the exact value of 0.01432 for an elliptically loaded isolated wing of aspect ratio 8. Thus, the formation flight results in a nearly 50% reduction in total induced drag. These results from the current approach are identical to those presented in Ref. 4.

Although the formation C_{Di} and the optimum downwash and lift distributions are all independent of the streamwise separation X, the distribution of the induced drag among the three wings does depend on the value of X. When $X = 3b$, the values of the individual aircraft C_{Di} are 0.01478 for the lead wing and 0.00322 for each of the two trailing aircraft. Thus, at this large streamwise separation, the formation flying results in a large benefit to the two trailing aircraft while slightly penalizing the lead aircraft. At a much smaller streamwise separation of $X = 0.25b$, the benefits are slightly more equally distributed, with the individual aircraft C_{Di} being 0.01356 for the lead aircraft and 0.00383 for the two trailing aircraft. For negative values of X, when the middle aircraft trails behind the two corner aircraft, the middle aircraft can experience an induced thrust. For example, when $X = -2b$, the values for the individual aircraft C_{Di} are -0.00642 for the middle aircraft and 0.01382 for each of the two corner aircraft. In all three cases, it is seen that the average C_{Di} is 0.00707. These trends agree with those presented in Ref. 4.

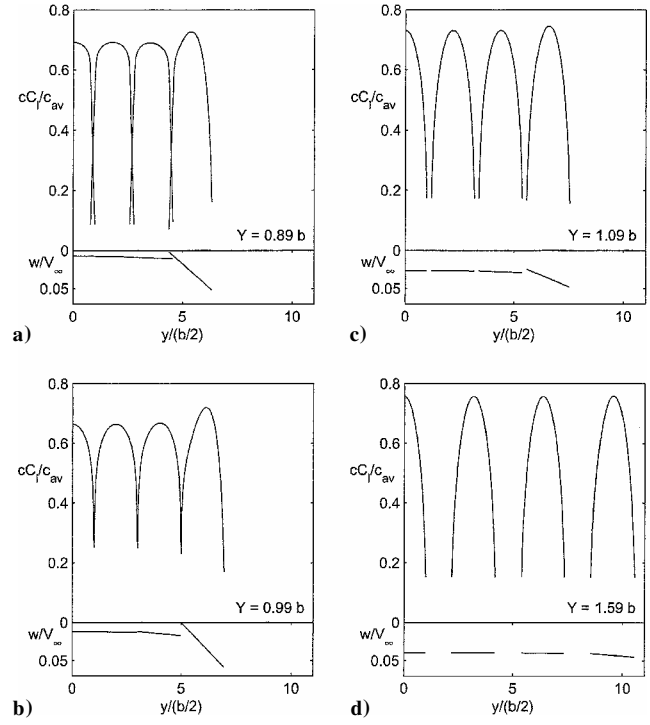

Fig. 3 Effect of lateral spacing on the optimum lift and Trefftz-plane downwash distributions for the seven-aircraft example: a) $Y = 0.89b$, b) $Y = 0.99b$, c) $Y = 1.09b$, and d) $Y = 1.59b$.

Figures 3a–3d show the results of the current method applied to symmetric formation flight of seven identical wings, each flying at C_L of 0.6 with zero rolling moment. All of the wings have an aspect ratio of 8. There is a small vertical separation of 1% span between two adjacent wings. This study shows the sensitivity of the optimum downwash, lift distribution, and total induced drag to lateral spacing of the aircraft. For small lateral separation (Fig. 3a), note that the optimum lift distribution for each wing deviates significantly from an elliptic distribution. As the aircraft are spaced farther away laterally from each other, the optimum loading becomes closer to the single-aircraft optimum elliptic loading, and the downwash distribution becomes closer to a constant along the span. The total induced drag reduction compared to solo flight is highest (71%) for the smallest lateral spacing (Fig. 3a). With progressive increase in the lateral spacing, the induced drag reduction decreases to 63, 38, and 14%, respectively for Figs. 3b, 3c, and 3d. These trends are, in general, consistent with those reported in Ref. 4 and the flight-test results of Ref. 3.

Conclusions

The calculus-of-variations approach previously used by Jones[6] for determining minimum induced drag of single wings has been extended to handle multiple wings in formation flight with constraints on the lift and rolling moment for each wing. The approach shows that the lift distributions for wings in formation flight with constraints on the lift and rolling moment on each wing must result in a linear variation in the Trefftz-plane downwash for the total induced drag of the formation to be a minimum. This simple and elegant result illustrates the power of the optimum-downwash approach pioneered by Munk[5] and Jones.[6] The optimum lift distribution was obtained from the optimum downwash using a discrete vortex lattice method similar to that described by Blackwell.[8] The results from the current approach agree identically with those obtained using a constrained-minimization approach.[4] The current approach considers only wings in formation flight and needs to be extended to handle aircraft in formation, with each aircraft being in longitudinal trim, as was done in Ref. 4. Additionally, like the constrained-minimization approach,[4] the current formulation is also valid only for formation geometries in which the wake traces of the

wings in the Trefftz plane do not intersect or overlap with each other. Although there does not appear to be any significant computational advantage to the present method when compared to that of a constrained-minimization technique,[4] the present method provides a simple closed-form expression for the optimum downwash and, thus, provides additional insight into the aerodynamics of ideal formation flight.

References

[1]Lissaman, P. B. S., and Shollenberger, C. A., "Formation Flight of Birds," *Science*, Vol. 168, No. 3934, May 1970, pp. 1003–1005.

[2]Weimerskirch, H., Martin, J., Clerquin, Y., Alexandre, P., and Jiraskova, S., "Energy Saving in Flight Formation," *Nature*, Vol. 413, No. 6857, Oct. 2001, pp. 697–698.

[3]Vachon, M. J., Ray, R. J., Walsh, K. R., and Ennix, K., "F/A-18 Aircraft Performance Benefits Measured During The Autonomous Formation Flight Project," AIAA Paper 2002-4491, Aug. 2002.

[4]Iglesias, S., and Mason, W. H., "Optimum Spanloads in Formation Flight," AIAA Paper 2002-0258, Jan. 2002.

[5]Munk, M. M., "The Minimum Induced Drag of Aerofoils," NACA Rept. 121, 1921.

[6]Jones, R. T., "The Spanwise Distribution of Lift For Minimum Induced Drag of Wings Having a Given Lift and a Given Bending Moment," NACA TN 2249, Dec. 1950.

[7]Jones, R. T., and Lasinski, T. A., "Effect of Winglets on the Induced Drag of Ideal Wing Shapes," NASA TM 81230, Sept. 1980.

[8]Blackwell, J. A., Jr., "Numerical Method to Calculate the Induced Drag or Optimum Loading for Arbitrary Non-Planar Aircraft," NASA SP 405, May 1976.

[9]Rossow, V. J., "Lift-Generated Wakes of Subsonic Transport Aircraft," *Progress in Aerospace Sciences*, Vol. 35, No. 6, pp. 507–660.

Validation of a Wall Interference Correction Procedure in Subsonic Flow

G. Lombardi* and M. V. Salvetti†
University of Pisa, 56123 Pisa, Italy
and
M. Morelli‡
CSIR, Pretoria 0001, South Africa

Introduction

ONE of the main sources of error affecting the experimental measurements of the flowfield around a model is the interference effects of wind-tunnel walls. Classical correction criteria are based on theoretical linear models, and thus, their validity is limited. More recently, new correction methods were introduced. (For a general description, see Ref. 1.) These methods are based on more complex procedures that couple measurements, typically pressure and/or velocity on the wall or in the field, with numerical calculations.

A method of correction for the wall interference effects was developed, based on pressure measurements on the wind-tunnel walls coupled with a numerical procedure to evaluate the flow correction, which is described in detail in Refs. 2 and 3.

Received 15 November 2002; revision received 17 March 2003; accepted for publication 29 March 2003.

*Associate Professor, Department of Aerospace Engineering. Member AIAA.

†Associate Professor, Department of Aerospace Engineering.

‡Senior Engineer, Medium Speed Wind Tunnel.

A preliminary application of the setup methodology to the correction of the aerodynamic coefficients of a complete aircraft model in subsonic conditions was described in Ref. 3. The results were compared with those obtained with a pretest correction method, and a satisfactory agreement was obtained. Clearly, this cannot be considered as a definitive validation of the correction procedure.

In the present paper, the methodology is applied to real experimental data, therefore, as a posttest procedure. Experiments on a complete aircraft configuration have been carried out using two different model sizes. The use of different scale models, operating in a given wind tunnel under identical flow conditions, appears to be the most appropriate procedure to gain information on the validity of the proposed correction procedure. Indeed, this approach gets rid of all differences related to the free-stream flow conditions, and the uncertainty in measurement comparisons is considerably reduced, being limited to the random component (which can be reduced, theoretically, to any desired value) of the measurement procedure.

Subsonic and low-angle-of-attack conditions have been considered. These can be considered the most critical conditions for the correction procedure; indeed, they are characterized by low wall interference effects, and this leads to a great sensitivity to the measurement uncertainty (both for the forces and the wall pressure). Therefore, it is anticipated that the correction procedure is more accurate the more important the wall effects to be corrected are.

Description of the Correction Procedure

The adopted correction methodology is a so-called posttest procedure[4]; in this kind of method, experimental data must be provided on a control surface located near the wind-tunnel walls or directly on them. In particular, a one-array correction procedure has been chosen, in which pressure data are provided at some locations on the wind-tunnel walls. The correction methodology employed and the sensitivity analysis carried out to study the effects of different pressure sensors position and accuracy are described in Ref. 2.

The scheme of the correction procedure, which is based on the method proposed by Sickles,[5] is shown in Fig. 1. Once the model geometry is defined, the experimental tests are carried out, and in addition to the aerodynamic forces acting on the model, the pressure over the wind-tunnel walls is measured at a few selected locations. These measurements are used as boundary conditions in a numerical simulation of the flow around the same geometry (pressure-given simulation). Another numerical simulation is carried out in free-air conditions, that is without the presence of solid walls. The difference between the values of aerodynamic forces obtained in these two simulations is used to correct the experimental data.

For the choice of the flow solver adopted in the numerical simulations, the same criteria used in computational aerodynamics are clearly suitable also in this context. In the present paper subsonic flow conditions at low angles of attack are considered, and thus, a potential flow solver is used.[6] It is based on Morino's formulation, with a wake relaxation procedure and has been extensively validated for aircraft configurations (for instance, see Ref. 7).

Experimental Setup

The experimental setup has been described in detail in Ref. 8. Tests are carried out in the high speed wind tunnel (HSWT) of the CSIR Laboratories. The HSWT is a trisonic, open circuit blow down-type tunnel. Its operational speed ranges from $M = 0.55$ to $M = 4.3$ The test section has a 0.45×0.45 m square section, and the length is 0.9 m.

The Mirage F1 model, a wing–tail configuration with moderate aspect ratio (2.83), was selected because of availablity in different scales: 1:32, and 1:40. The nominal blockage factors, defined as the ratio between the model cross-sectional area and the test section area, at zero angle of attack, are 0.0101 for the 1:40 model and 0.0158 for the 1:32 model, whereas the span/width ratios are 0.210 and 0.263, respectively.

The aerodynamic forces are nondimensionalized with the dynamic pressure and the wing planform area, whereas the reference